Proc. Natl. Acad. Sci. USA
Vol. 93, pp. 10338–10342, September 1996
Immunology

Shared fine specificity between T-cell receptors and an antibody recognizing a peptide/major histocompatibility class I complex

ANETTE STRYHN*, PETER S. ANDERSEN†, LARS Ø. PEDERSEN*, ARNE SVEJGAARD‡, ARNE HOLM§, CHRISTOPHER J. THORPE¶, LARS FUGGER‡, SØREN BUUS*, AND JAN ENGBERG†‖

*Department of Experimental Immunology, Institute of Medical Microbiology and Immunology, Panum 18.3.22, University of Copenhagen, Blegdamsvej 3C, DK-2200 Copenhagen N, Denmark; †Department of Biological Sciences, The Royal Danish School of Pharmacy, Universitetsparken 2, DK-2100 Copenhagen Ø, Denmark; ‡Department of Clinical Immunology, National University Hospital, Tagensvej 20, DK-2200 Copenhagen N, Denmark; §Chemistry Department, Royal Veterinary and Agricultural University, Thorvaldsensvej 40, 1871 Frederiksberg C, Copenhagen, Denmark; and ¶Department of Crystallography, Birkbeck College, Malet Street, London WC1E 7HX, United Kingdom

Communicated by Hans H. Ussing, University of Copenhagen, Copenhagen, Denmark, July 2, 1996 (received for review April 24, 1996)

ABSTRACT **Cytotoxic T cells recognize mosaic structures consisting of target peptides embedded within self-major histocompatibility complex (MHC) class I molecules. This structure has been described in great detail for several peptide–MHC complexes. In contrast, how T-cell receptors recognize peptide–MHC complexes have been less well characterized. We have used a complete set of singly substituted analogs of a mouse MHC class I, K^k-restricted peptide, influenza hemagglutinin $(Ha)_{255-262}$, to address the binding specificity of this MHC molecule. Using the same peptide–MHC complexes we determined the fine specificity of two $Ha_{255-262}$-specific, K^k-restricted T cells, and of a unique antibody, pSAN, specific for the same peptide–MHC complex. Independently, a model of the $Ha_{255-262}$-K^k complex was generated through homology modeling and molecular mechanics refinement. The functional data and the model corroborated each other showing that peptide residues 1, 3, 4, 6, and 7 were exposed on the MHC surface and recognized by the T cells. Thus, the majority, and perhaps all, of the side chains of the non-primary anchor residues may be available for T-cell recognition, and contribute to the stringent specificity of T cells. A striking similarity between the specificity of the T cells and that of the pSAN antibody was found and most of the peptide residues, which could be recognized by the T cells, could also be recognized by the antibody.**

Eradicating infected cells is an important strategy in the defense against intracellular pathogens. One of the cell types involved, the $CD8^+$ cytotoxic T cells (CTLs), has developed a unique and quite elaborate mode of recognition: only antigens, which are presented in association with class I molecules of the major histocompatibility complex (MHC), are recognized (1). The function of MHC class I molecules is to sample peptides derived from the cytosolic protein environment of the target cell (reviewed in ref. 2). The MHC specifically selects some of these peptides, transports them to the target cell surface where they are presented to $CD8^+$ CTLs. Although additional accessory molecules are involved in the activation of T cells, the final antigen-specific event is thought to be the creation of multimeric complexes consisting of T-cell receptors (TcR) and peptide–MHC class I complexes (3).

MHC class I molecules are highly polymorphic heterodimers that consist of a transmembrane heavy chain and a noncovalently associated soluble light chain, the β_2-microglobulin (4). The majority of the polymorphism is concentrated in the membrane distal domains of the heavy chain, α_1 and α_2, which form a unique peptide-binding structure (5–8). X-ray crystallography has revealed this target structure to be a collage in which the peptide is deeply buried within the MHC. This leaves only a minority of the peptide residues, scattered and intermingled with MHC residues, available for T-cell recognition (reviewed in ref. 9). The specificity of peptide–MHC interactions has been described in great detail, whereas little biochemical (10–14) or structural (15, 16) data exist on T-cell recognition. It is generally assumed that self-MHC accounts for the majority of the T-cell target structure, whereas antigenic peptides constitute a smaller, albeit highly heterogeneous portion of this structure (8, 17). The peptide is at the center of the MHC target structure (5), and it is assumed that this is appositioned by the most diverse part of the TcR, the CDR3 regions (17). Further assuming that the TcR structure bears some resemblance to antibody structures, models have placed the CDR3 regions in the center of the TcR (17). Structural data support this model (16). Thus, the core regions of the peptide–MHC and the TcR structures are thought to align to afford an extensive surface overlap, but the orientation of the TcR relative to the MHC is controversial (12, 18).

We have used a complete set of singly substituted analogs of a CTL epitope to examine the fine specificity of the mouse MHC class I molecule, K^k. Independently, we have generated a model of the peptide–MHC complex. Furthermore, we have examined the fine specificity of two T cells specific for this particular peptide–MHC complex and examined the fine specificity of a unique antibody specific for the same peptide–MHC complex. The TcR and the antibody appeared to recognize almost identical target structures, with peptide contributions being donated by all by non-primary anchor residues.

MATERIALS AND METHODS

Cells. The AKR ($H\text{-}2^k$)-derived T-cell lymphoma, RDM-4, was used for production of K^k (19, 20). The influenza (ATCC VR100) hemagglutinin $(Ha)_{255-262}$ (FESTGNLI, single-letter amino acid code)-specific, K^k-restricted T-cell hybridomas, HK8.3-5H3 and HK8.3-6F8 have been described (21).

Antibodies. The monoclonal antibody 11-4-1 [anti $\alpha_{1\text{-}2}$ K^k, (22)] was produced as ascites and purified by protein-A Sepharose (Pharmacia) affinity chromatography. The generation of the $Ha_{255-262}$-specific, K^k-restricted recombinant Fab antibody fragment, pSAN13.4.1, has been described (23).

Peptides. A complete (except cysteine) set of single substituted analog peptides was synthesized for the $Ha_{255-262}$ (FESTGNLI) epitope by standard fluorenylmethoxycarbonyl (Fmoc) protection strategy using a multi-peptide synthesizer (24).

MHC Purification, Peptide–MHC Binding, MHC Specificity. K^k molecules were affinity-purified from lysates of RDM-4 using 11-4-1 coupled to cyanogen bromide-activated Sepharose 4B as the affinity matrix (20). To determine the specificity

The publication costs of this article were defrayed in part by page charge payment. This article must therefore be hereby marked "*advertisement*" in accordance with 18 U.S.C. §1734 solely to indicate this fact.

Abbreviations: MHC, major histocompatibility complex; TcR, T-cell receptor; IL-2, interleukin 2; CTL, cytotoxic T cells.

‖To whom reprint requests should be addressed.

of the K^k molecule we used a biochemical peptide–MHC binding assay (25).

T-Cell Hybridoma Stimulation, TcR Specificity. An *in vitro* stimulation assay was used to determine the fine specificity of the $Ha_{255-262}/K^k$ specific T-cell hybridomas (21). RMA-K^k (a K^k transfected thymoma), was used as antigen presenting cell. RMA-K^k (1×10^5 per well) were incubated with 1×10^5 of the $Ha_{255-262}$-specific, K^k-restricted hybridomas, HK8.3-5H3 or HK8.3-6F8 in a 96-well microtiter plate. Graded concentrations of the $Ha_{255-262}$ peptide, or analog substitutions hereof, were added and the cultures incubated for 24 h in RPMI 1640 medium supplemented with 10% FCS at 37°C in a humidified atmosphere containing 5% CO_2/95% air. Supernatants were harvested and tested for interleukin 2 (IL-2) content using 4000 per well of the IL-2-dependent cell line, HT-2, as originally described by Kappler *et al.* (26). The concentration of peptide needed to obtain 100 units/ml of IL-2 was determined.

Specificity of the Recombinant pSAN13.4.1 Antibody. Specific $Ha_{255-262}$-K^k complexes were generated, purified, and coated at a suboptimal concentration of 10 pg (10 nM) per well onto Maxisorp (Nunc) 96-well flat-bottom microtiter plates. The plates were subsequently blocked in 2% skimmed milk in PBS buffer and then exposed to pSAN13.4.1 expressed as a fusion protein at the end of pIII of the filamentous phage. The plates were washed, exposed to horseradish peroxidase-coupled anti-phage antibodies (Pharmacia), washed, developed, and read in an ELISA reader at 490 nM. To determine the fine specificity of pSAN13.4.1, graded concentrations of analog–K^k complexes (generated with 450 μM of analog to effect K^k-saturation) were added as competitors prior to addition of pSAN13.4.1 phages. The concentration of competitor complex needed to effect 50% inhibition (the IC_{50}) was determined. The lower the IC_{50} the stronger the binding of the pSAN13.4.1 to the analog–K^k complex.

Molecular Modeling of the $Ha_{255-262}$-K^k Complex. A molecular model for the K^k molecule was constructed from the vesicular stomatitis virus NP_{50-57}-K^b crystallographic structure (8) using the COMPOSER homology modeling package implemented within SYBYL 6.0 molecular modeling software (Tripos Associates, St. Louis), using previously described protocols (27).

RESULTS

MHC Class I K^k Recognition of the $Ha_{255-262}$ Epitope. To determine the specificity of K^k, we synthesized and examined a complete set of singly amino acid substituted peptide analogs of the K^k-restricted, CTL epitope from influenza virus hemagglutinin, $Ha_{255-262}$ (FESTGNLI). For every position within this epitope, the parental amino acid was replaced one by one with each of the other naturally occurring amino acids (except cysteine). These analogs were tested for K^k binding in a biochemical inhibition assay (25) and the effect of each substitution was expressed as $-\log[IC_{50}(\text{analog})]$ (Fig. 1*A*). Strikingly, the majority of the substitutions were more or less accepted by K^k. In particular, K^k appeared indifferent to substitutions in positions 3, 4, and 6 as none of the substitutions at these positions led to significant changes in K^k binding. Only 14 (or 10%) of the 144 substitutions led to more than a 100-fold drop in binding. These deleterious substitutions were entirely concentrated in positions 2 and 8, which preferred the amino acids E and I, respectively. Our data suggest that position 8 is the most critical of the two since 9 substitutions led to a more than 10-fold drop in binding compared to only 6 substitutions at position 2. Less pronounced effects of substitutions were

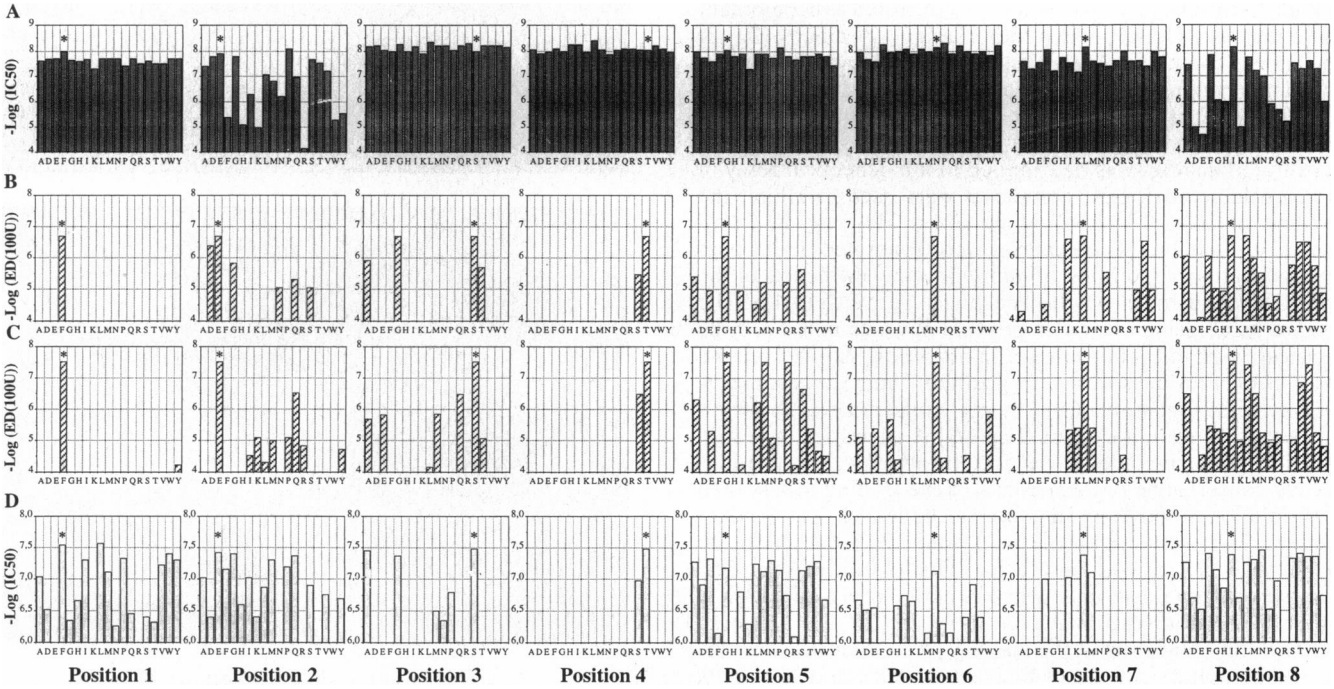

FIG. 1. The fine specificities involved in $Ha_{255-262}$-K^k recognition. Singly substituted analogs of the $Ha_{255-262}$ peptide were tested for binding to K^k, for stimulation of the two T cells, and for binding to the antibody pSAN13.4.1. (*A*) Specificity of K^k. The concentration of analog peptide needed to inhibit the binding of radiolabeled NP_{50-57} to purified K^k by 50% (the IC_{50}) was determined. This was reported as the negative logarithm of the IC_{50}. (*B* and *C*) Specificity of HK8.3-5H3 and HK8.3-6F8. RMA-K^k (10^5), HK8.3-5H3 (10^5) (*B*) or HK8.3-6F8 (10^5) (*C*), and graded concentrations of $Ha_{255-262}$ were incubated at 37°C in 96-well microtiter plate wells. Supernatants were harvested 24 h later and tested for IL-2 content using the IL-2 dependent cell line HT-2. The concentration of peptide analog leading to the secretion of 100 units/ml of IL-2 (the ED_{100}) was determined. (*D*) Specificity of pSAN13.4.1. pSAN13.4.1 was mixed with graded concentrations of K^k saturated with one of the various analog peptides and incubated in 96-well microtiter plates, which had been precoated with a suboptimal concentration of $Ha_{255-262}$-K^k complexes. Bound pSAN13.4.1 was detected with horseradish peroxidase-coupled anti-phage antibodies (Pharmacia), washed, developed, and read in an ELISA reader at 490 nM. The concentration of peptide analog leading to IC_{50} was determined.

found for positions 1, 5, and 7, where F appeared to be preferred in position 1, charged amino acids and Y to be disfavored in position 5, and F and L to be preferred in position 7.

T-Cell Recognition of the K^k-Restricted $Ha_{255-262}$ Epitope. To examine the fine specificity of MHC class I restricted T-cell responses, the stimulatory capacities of each of the single amino acid substituted analogs were determined in a bioassay using the two $Ha_{255-262}$ specific, K^k-restricted T-cell hybridomas, HK8.3-6F8 (Fig. 1*B*) and HK8.3-5H3 (Fig. 1*C*). It should be noted that this assay depends on both K^k binding and T-cell recognition. A dose-response analysis was made for each analog and used to determine the concentration of analog needed to stimulate a response of 100 units/ml of IL-2. The most critical peptide residues were F in position 1 (both hybridomas), T in position 4 (both hybridomas), and N in position 6 (HK8.3-6F8). In these positions, the T-cell specificities were very stringent as only the parental amino acids were accepted; any substitution led to a complete loss of stimulatory activity (except for the conservative substitution of T → S in position 4, which led to a 10-fold loss). Considerable, but less stringent, specificity was observed for position 3 (both hybridomas), position 6 (HK8.3-5H3), and position 7 (both hybridomas). Only a few substitutions, mostly conservative or semi-conservative, were allowed in these positions. A slightly more promiscuous specificity was observed for position 5 (both hybridomas). Finally, the least critical peptide residues were the anchor positions for K^k: I in position 8 (both hybridomas) followed by E in position 2 (both hybridomas). Several substitutions were more or less accepted in these positions, and many of the substitutions, which led to a loss of T-cell stimulatory activity, could be accounted for by loss in K^k binding.

Recognition of the K^k-Restricted $Ha_{255-262}$ Epitope by a "T cell like" Antibody. We have recently generated a recombinant antibody, pSAN13.4.1, with a rather unique specificity (23). It recognizes complexes consisting of $Ha_{255-262}$ and K^k in a way that appears reminiscent of a peptide-specific, MHC-restricted T-cell specificity. To further investigate this point, the pSAN13.4.1-binding capacity of each of the single amino acid substituted analogs was determined in a biochemical assay in which soluble analog–K^k complexes were used to inhibit the binding of pSAN13.4.1 to immobilized $Ha_{255-262}$–K^k complexes. The analog–K^k complexes were generated under peptide-saturating conditions to minimize the influence of K^k specificity and focus on the specificity of pSAN13.4.1. The most critical residue was T in position 4, which could only be replaced with the conservative substitution, S. The second most critical residues were L in position 7 and S in position 3, where some substitutions, mostly conservative to semi-conservative, were accepted (Fig. 1*D*). Less critical was F in position 1, which could be replaced by about 10 substitutions mostly conservative or semi-conservative leading to less than a 10-fold loss in binding. In contrast, the less critical residues were G in position 5 and E in position 2, which could be replaced by 13 or 14 amino acids. Finally, the least critical residue was I in position 8, which could be replaced with any other amino acid (except R).

Molecular Modeling of the $Ha_{255-262}$ K^k Complex. Since the crystallographic structure of K^k has not yet been determined, we have used homology modeling of the K^k molecule to obtain a structural representation of the molecule, in an attempt to analyze the peptide-binding preferences of the molecule and the recognition of the $Ha_{255-262}$–K^k complex. In terms of sequence identity, the K^b molecule is closely related to the K^k molecule, and because K^b has already been analyzed structurally using x-ray crystallography, it was selected as a template structure for the K^k model. Comparing the K^k model to the K^b crystallographic structure highlights some interesting similarities and differences in cleft architecture (Fig. 2 *A* vs. *B*). The K^k molecule has a deep hydrophobic invagination at the location within the cleft, which is responsible for binding the side chain of the C-terminal amino acid of the peptide. This pocket is almost identical in shape and chemical nature to the equivalent pocket in the K^b molecule, explaining the similar binding capacities of the two molecules in the class of the C-terminal anchor selected. However, the deep pocket in the K^b molecule, which sequesters the central P5 anchor of K^b binding peptides, is completely occluded in the K^k molecule, where the P5 glycine "side chain" rests on a plateau in the center of the cleft. This suggests that side chains of P5 of K^k binding peptides either face outward, or if facing downward into K^k side, are limited to only the smallest amino acids, such as glycine and alanine.

DISCUSSION

To distinguish between the direct effect of amino acid substitutions within the K^k-restricted peptide, FESTGNLI, on T-cell and antibody recognition, and secondary effects caused by a change in MHC binding capacity, we analyzed the ability of a panel of singly substituted analogs to bind to the K^k molecule. This analysis confirmed previous assignments of positions 2

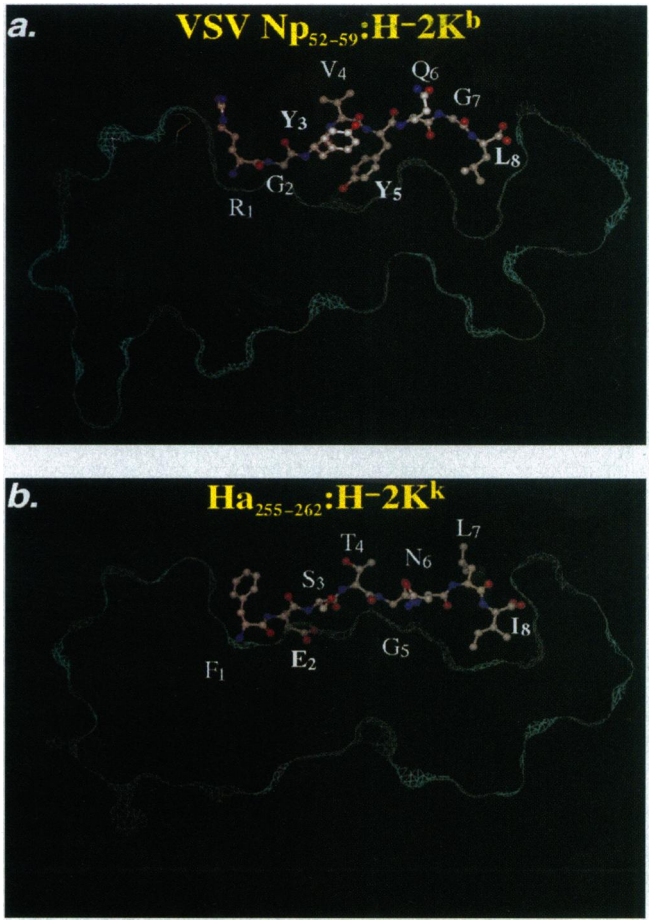

FIG. 2. Comparison of the cleft architectures of K^b and K^k. (*a*) Structure of K^b binding the vesicular stomatitis virus NP_{52-59} peptide (RGYVYQGL) (8). (*b*) Model of K^k binding the $Ha_{255-262}$ peptide (FESTGNLI). In both *a* and *b* the peptide runs N terminally to C terminally, left to right, through the cleft. The green mesh Connolly surface is sliced 1 Å thick, and the slice displayed is positioned in a plane along the Z-axis at which maximal peptide:MHC contact occurs. The color coding for atoms is as follows: carbon, white; nitrogen, blue; oxygen, red. The complimentarity of anchoring peptide side chain shape, and the size and shape of the specificity pocket in which they are sequestered, is clear in this view. Images were produced using INSIGHT II (Biosym).

(E) and 8 (I) as anchor residues (28, 29). Subsequently, we investigated the specificity of two $Ha_{255-262}$-specific, K^k-restricted T-cell hybridomas. The vast majority of the single substitutions (≈70%) completely destroyed the epitope as seen by both hybridomas, ≈20% led to a pronounced, albeit not complete, loss of stimulation and only ≈10% led to less than a 10-fold loss in stimulatory capacity. In accordance with previous observations on T-cell specificity (30–33), the present hybridomas exhibited an exquisite specificity as most singly substitutions, even conservative ones, were detectable; the few more or less acceptable substitutions tended to be conservative: E → D, S → A, T → S, G → A, L → I/V, etc. The two T hybridomas had largely overlapping specificities; however, there were also distinct differences between the two (e.g., D and G in position 2; E, G, M, Q in position 3; several amino acids in position 6; P and V in position 7). The most important positions in shaping the T-cell specificity were readily identified as positions 1, 4, and 6 where very few, if any, substitutions were allowed. Slightly less important were positions 3 and 7 followed by the intermediary position 5. Position 8 was clearly the least important residue in defining the T-cell specificity, and taking the requirement for K^k interaction into account, position 2 did not appear important either. These data would suggest that the TcRs interact with the specific side chains of the residues corresponding to positions 1, 4, and 6, thus requiring absolute amino acid identity at these positions. Less stringent requirements are placed upon positions 3 and 7, which could be explained by the T-cell receptor crossreacting with a few (mostly structurally similar) side chains. The lack of specificity corresponding to positions 8, 2, and 5 could be due to the TcR not interacting with these side chains, or interacting with the peptide backbone (i.e., no requirement for amino acid identity). In terms of availability, our data would suggest that the side chains of positions 1, 4, and 6 are accessible to the receptors, pointing out of the peptide binding cleft, or at least sideways. The side chains of positions 3 and 7 are also to some extent accessible. The side chains of positions 8 and 2 are inaccessible, most likely because they point into the MHC, in accord with their assignment as primary anchors. Note that the assignment of positions 1, 4, and 6/7 as T-cell interacting positions correspond as a mirror image to the assignment of positions 2 and 8 (and to some extent 5) as MHC interacting positions, so that recognition of the same amino acids by both TcR and MHC class I does not appear to occur, at least not for these hybridomas. In contrast, one of us (S.B.) has previously suggested such corecognition in a mouse MHC class II system (30).

We generated pSAN13.4.1 through recombinant technology involving selection from a phage-display library (23). The specificity of pSAN13.4.1 resembled that of $Ha_{255-262}$-specific, K^k-restricted T cells because it only recognized $Ha_{255-262}$ in the context of K^k and, furthermore, resulted in specific and potent inhibition of specific T-cell responses. Now we have examined the fine specificity of pSAN13.4.1 and compared it to the specificity of two T-cell responses. As illustrated in Fig. 1, a striking similarity was found between the specificities of the two TcRs and that of pSAN13.4.1. Thus, the $Ha_{255-262}$ positions 4 and 7, followed by positions 3 and 6, were recognized with high stringency by pSAN13.4.1. These results illustrate that antibodies can mimic, and potentially assume, structures similar to TcRs. The major difference between the recombinant antibody and the TcRs was observed at position 1 where the antibody largely ignored this residue, whereas both T cells crucially depended on its identity. This may indicate that the antibody and the TcRs, despite their use of similar contact points around the center of the MHC-bound peptide, have slightly different orientations relative to the MHC molecule resulting in a different requirement for recognition of the N terminus of the peptide.

A theoretical model of the $Ha_{255-262}$–K^k complex was build independently of the experimental result. This model suggests that the peptide lies in an irregular extended conformation. The N terminus of the peptide is completely buried within the A pocket, but its phenylalanine side chain extends to the surface of the MHC, and may be seen obliquely from the direction of the α_2-helix. The side chain of the glutamic acid residue in the anchoring position 2 is completely buried in the B pocket. The side chain of the serine in position 3 is pointing sideways and up towards the α_2-helix of the MHC. The side chain of the threonine in position 4, in addition to leucine in position 7, point straight up and are the most accessible residues in the peptide, in keeping with the T-cell stimulation and pSAN13.4.1 recognition data. In contrast, the "side chain" of the glycine in position 5 is buried, laying upon a plateau that traverses the cleft of the K^k molecule, with the Cα carbon, the point of attachment for peptide side chains, facing downwards. The side chain of the asparagine in position 6 points sideways towards the α_2-helix and is partially exposed permitting recognition by the TcR. Finally, the side chain of the isoleucine in position 8 is deeply embedded in the F pocket. The data on the recognition of the analogs by K^k show that two of the three peptide side chains, which the model suggests are pointing downwards, are actively involved in MHC interaction. Similarly, the data on the T-cell and pSAN13.4.1 recognitions demonstrate that all of the peptide side chains, which the model suggests are pointing upwards, are actively involved in TcR or pSAN13.4.1 interaction. These independent observations provides an excellent validation for the model of the $Ha_{255-262}$–K^k complex presented here.

The experimental results and the model contribute to our understanding of T-cell specificity and structure. Our data support the assumption that the structure of the TcR resembles that of an immunoglobulin Fab fragment (15–17). Thus, the TcR would engage a surface area of ≈800 Å^2, much like the size and shape the $Ha_{255-262}$–K^k complex as it is outlined in Fig. 3*a*. The peptide only contributes a minor proportion of the total ligand surface. This outward facing surface of the peptide–MHC complex appears quite flat with minor indentions notably between the α-helices and the peptide, leaving some of the sideways pointing residues accessible (Fig. 3 *b–d*). Most of the peptide side chains did not extend above the plane of the α-helices. Nonetheless, the identity of these side chains can be detected by the TcRs, suggesting that the side chains of the variable loops of the TcR may interdigitate into the cleft and contact the semi-exposed side chains of the peptide. Recently, TcRs have been reported to recognize different core regions of the peptide–MHC complex, e.g., either centered around the N- or C-terminal part of the peptide (34). In contrast, we find that both T cells recognize the peptide from the N terminal of the peptide and almost to the C terminal, and that the TcR must interact with the majority, if not all, of the available side chains. Thus, the TcR appears to make the most of the relatively minor contribution of the peptide to the overall ligand surface. As the majority of the TcR ligand is made up of self-MHC, maximizing the contribution of the peptide should make it easier for the T cells to distinguish between self and non-self. This feat, however, cannot be a simple one since T cells must be educated in the thymus through positive and negative selection processes to become self-MHC restricted, i.e., to exhibit a certain measure of self-reactivity, yet avoid excessive self-reactivity. In contrast, antibodies are not educated to be self-MHC restricted and consequently "T cell like" antibodies should be rare. In agreement, such antibodies have only been sporadically reported in the literature and we had to resort to the high-selection power of the phage display technology to identify an MHC-restricted antibody. If antibodies and TcRs are structurally related, then the difference in recognition between antibodies and TcRs may be the result of the educational processes during the development of the two

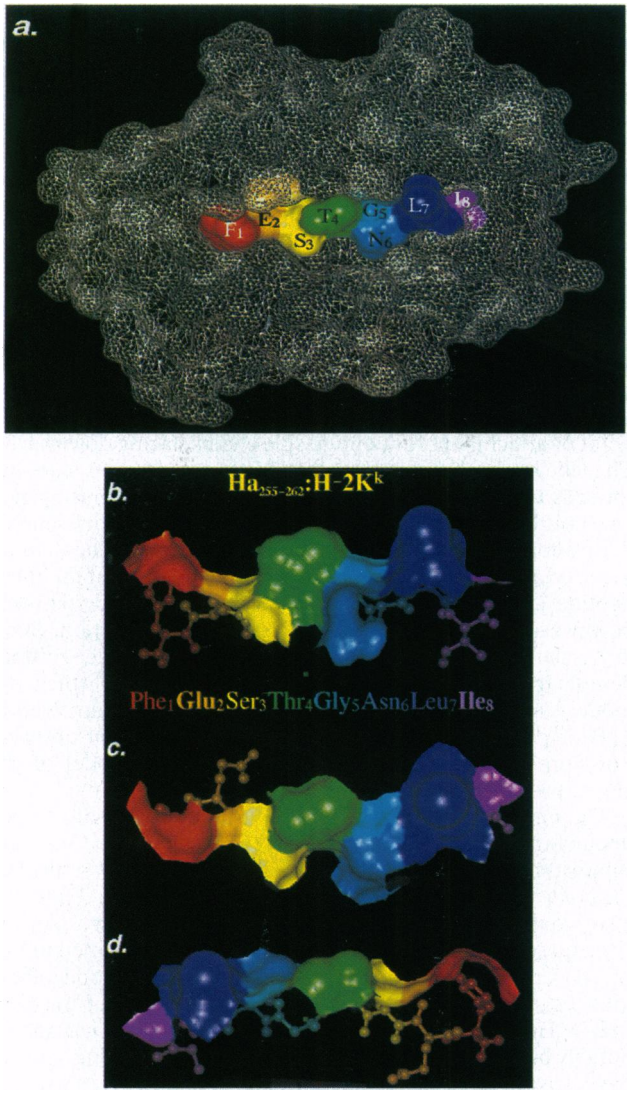

FIG. 3. The TcR accessible part of the MHC-bound peptide. One top view (*a*) of the $Ha_{255-262}$–K^k complex presented to T cells. The peptide is colored as for Fig. 2, whereas the MHC is white. Also shown are two orthogonal views (*b* and *d*), and a top view (*c*) of the $Ha_{255-262}$ peptide bound to K^k in which only the portion of the solvent accessible surface of the complex, which belongs to the peptide, is displayed. Images were produced using INSIGHT II (Biosym).

responses. Evolutionary, the segregation between the two recognition modes may be more functionally than structurally determined.

We thank Dr. Michael Gajhede at the Chemical Institute, University of Copenhagen, for letting us use their facility for the molecular modeling. S.B., L.F., and A.S. are members of the Biotechnology Center for Signal Peptide Research (now Center for Cellular Communication) and S.B. is a member of the Center for Medical Biotechnology. C.J.T. is a Fullbright Cancer Scholar and Louise Buchanan Cancer Fellow. This work was supported by the Danish Medical and Natural Sciences Research Council, the Carlsberg Foundation, the Novo–Nordisk Foundation, the Danish Multiple Sclerosis Foundation, and the Alfred Benzon Foundation.

1. Zinkernagel, R. M. & Doherty, P. C. (1974) *Nature (London)* **248,** 701–702.
2. Yewdell, J. W. & Bennick, J. R. (1995) *Adv. Immunol.* **52,** 1–123.
3. Janeway, C. A. & Bottomly, K. (1994) *Cell* **76,** 275–285.
4. Springer, T. A., Robb, R. J., Terhorst, C. & Strominger, J. L. (1977) *J. Biol. Chem.* **252,** 4694–4700.
5. Björkman, P. J., Saper, M. A., Samaoui, B., Bennett, W. S., Strominger, J. L. & Wiley, D. C. (1987) *Nature (London)* **329,** 506–512.
6. Björkman, P. J., Saper, M. A., Samraoui, B., Bennett, W. S., Strominger, J. L. & Wiley, D. C. (1987) *Nature (London)* **329,** 512–518.
7. Madden, D. R., Gorga, J. C., Strominger, J. L. & Wiley, D. C. (1991) *Nature (London)* **353,** 321–325.
8. Fremont, D. H., Matsumura, M., Stura, E. A., Peterson, P. A. & Wilson, I. A. (1992) *Science* **257,** 919–927.
9. Madden, D. R. (1995) *Annu. Rev. Immunol.* **13,** 587–622.
10. Schneck, J., Maloy, W. L., Coligan, J. E. & Margulies, D. H. (1989) *Cell* **56,** 47–55.
11. Matsui, K., Boniface, J. J., Reay, P. A., Schild, H., Fazekas de St. Groth, B. & Davis, M. M. (1991) *Science* **254,** 1788–1791.
12. Jorgensen, J. L., Esser, U., Fazekas de St. Groth, B., Reay, P. A. & Davis, M. M. (1992) *Nature (London)* **355,** 224–230.
13. Corr, M., Slanetz, A., Boyd, L. F., Jelonek, M. T., Khilko, S., Basel, K. A.-R., Kim, Y. S., Maher, S. E., Bothwell, A. L. M. & Margulies, D. H. (1994) *Science* **265,** 946–947.
14. Matsui, K., Boniface, J. J., Steffner, P., Reay, P. A. & Davis, M. M. (1994) *Proc. Natl. Acad. Sci. USA* **91,** 12862–12866.
15. Bentley, G. A., Boulot, G., Karjalainen, K. & Mariuzza, R. A. (1995) *Science* **267,** 1984–1987.
16. Fields, B. A., Ober, B., Malchioidi, E. L., Lebedeva, M. I., Braden, B. C., Ysern, X., Kim, J.-K., Shao, X., Ward, E. S. & Mariuzza, R. A. (1995) *Science* **270,** 1821–1824.
17. Davis, M. M. & Björkman, P. J. (1988) *Nature (London)* **334,** 395–402.
18. Hong, S. C., Chelouche, A., Lin, R., Shaywitz, D., Braunstein, N. S., Glimscher, L. & Janeway, C. A. (1992) *Cell* **69,** 999–1009.
19. Herrmann, S. H. & Mescher, M. F. (1979) *J. Biol. Chem.* **254,** 8713–8716.
20. Olsen, A. C., Pedersen, L. Ø., Hansen, A. S., Nissen, M. H., Olsen, M., Hansen, P. R., Holm, A. & Buus, S. (1994) *Eur. J. Immunol.* **24,** 385–392.
21. Stryhn, A., Pedersen, L. Ø., Ortiz-Navarrete, V. & Buus, S. (1994) *Eur. J. Immunol.* **24,** 1404–1409.
22. Oi, V. T., Jones, P. P., Goding, J. W., Herzenberg, L. A. & Herzenberg, L. A. (1978) *Curr. Top. Microbiol. Immunol.* **81,** 115–127.
23. Andersen, P. S., Stryhn, A., Hansen, B. E., Fugger, L., Engberg, J. & Buus, S. (1996) *Proc. Natl. Acad. Sci. USA* **93,** 1820–1824.
24. Holm, A. & Meldal, M. (1989) in *Multiple Column Peptide Synthesis*, eds. Bayer, E. & Jung, G. (de Gruyter, Berlin), pp. 208–209.
25. Buus, S., Stryhn, A., Winther, K., Kirkby, N. & Pedersen, L. Ø. (1995) *Biochim. Biophys. Acta* **1243,** 453–460.
26. Kappler, J. W., Skidmore, B., White, J. & Marrack, P. (1981) *J. Exp. Med.* **153,** 1198–1214.
27. Thorpe, C. J. & Travers, P. J. (1996) *Molecular Modeling Studies of the Interaction of Peptides with Major Histocompatibility Complex Class I and II Molecules* (IRL, Oxford).
28. Cossins, J., Gould, K. G., Smith, M., Driscoll, P. & Brownlee, G. G. (1993) *Virology* **193,** 289–295.
29. Norda, M., Falk, K., Rötzschke, O., Stefanovic, S., Jung, G. & Rammensee, H.-G. (1993) *J. Immunother.* **14,** 144–149.
30. Sette, A., Buus, S., Colon, S. M., Smith, J. A., Miles, C. & Grey, H. M. (1987) *Nature (London)* **328,** 395–399.
31. Suhrbier, A., Rodda, S. J., Ho, P. C., Csurhes, P., Dunckley, H., Saul, A., Geysen, H. M. & Rzepczyk, C. M. (1991) *J. Immunol.* **147,** 2507–2513.
32. Burrow, S. R., Rodda, S. J., Suhrbier, A., Geysen, H. M. & Moss, D. J. (1992) *Eur. J. Immunol.* **22,** 191–195.
33. Reay, P. A., Kantor, R. M. & Davis, M. M. (1994) *J. Immunol.* **152,** 3946–3957.
34. Nanda, N. K., Arzoo, K. K., Geysen, H. M., Sette, A. & Sercarz, E. E. (1995) *J. Exp. Med.* **182,** 531–539.